Journal of Molecular Catalysis A: Chemical 316 (2010) 118–125

Contents lists available at ScienceDirect

Journal of Molecular Catalysis A: Chemical

journal homepage: www.elsevier.com/locate/molcata

Review

Kinetics of the $H_2{}^{18}O/H_2{}^{16}O$ isotope exchange over vanadia–titania catalyst

E.M. Sadovskaya*, V.B. Goncharov, Yu.K. Gulyaeva, G.Ya. Popova, T.V. Andrushkevich

Boreskov Institute of Catalysis SB RAS, Lavrentieva str.5, 630090 Novosibirsk, Russia

ARTICLE INFO

Article history:
Received 10 June 2009
Received in revised form 6 October 2009
Accepted 6 October 2009
Available online 14 October 2009

Keywords:
^{18}O exchange
The water
Kinetics
Vanadia–titania catalyst

ABSTRACT

Study of oxygen exchange between vanadia–titania catalyst, H_2O and O_2 has been performed in isothermal (200 °C) and thermo programmed (50–500 °C) conditions. Experiments using $H_2{}^{18}O$, $^{18}O_2$ and monolayer vanadia–titania catalyst placed to the plug-flow reactor were carried out. Significant values of the rate of isotope exchange between O_2 and the catalyst were observed at $T > 450$ °C, but catalyst reduction accompanied oxygen desorption into gas phase proceeded in this case. Unlike dioxygen, water can exchange quite readily its oxygen atoms with vanadia–titania catalyst even at room temperature. Surface vanadium sites coordinating the *OH* group show the highest activity in the oxygen exchange with water. The rate constant of oxygen exchange between adsorbed water molecule and *V–OH* is ca. 0.5 s^{-1} at 200 °C, with the activation energy close to zero. The rate of oxygen exchange with dehydrated vanadium complexes *V–O–V* and *V=O* is much lower. The rate constant of this exchange is ca. 10^{-3} s^{-1} at 200 °C, with the activation energy of ca. 70 kJ/mol. The interaction of adsorbed water with VO_x species results in their slow hydrolysis to form the *V–OH* groups (characteristic time ca. 10^4 s), which recombination underlies the isotope exchange.

© 2009 Elsevier B.V. All rights reserved.

Contents

1. Introduction

In selective oxidation of hydrocarbons, there are many reactions where water has a considerable effect on the catalytic properties, various manifestations of such effect being reported in the literature. In the oxidation of 3-picoline on vanadia–titania catalyst, steam accelerates the formation of pyridine-3-carbaldehyde intermediate and subsequent formation of nicotinic acid, but has no effect on further oxidation of these products, and ultimately increases the catalyst activity and selectivity [1]. Steam is very effective in the oxidation of 3-picoline to nicotinic acid, 4-picoline to isonicotinic acid, and in the oxidation of 2-picoline to pyridine-3-carbaldehyde on *CrVP*-oxide catalyst [2–4]. When toluene is oxidized on vanadia–titania catalyst, the presence of water vapor provides a several-fold increase in the catalyst activity and enhances the selectivity for benzoic acid [5]. In distinction to the data reported in [5], in toluene oxidation on V_2O_5–Sb_2O_3/TiO_2, water does not facilitate the formation of benzoic acid, but has a

* Corresponding author.
E-mail address: sadovsk@catalysis.ru (E.M. Sadovskaya).

1381-1169/$ – see front matter © 2009 Elsevier B.V. All rights reserved.
doi:10.1016/j.molcata.2009.10.009

positive effect on selectivity for benzaldehyde and catalyst activity [6]. The facilitating effect of water was observed also in the reaction of butene oxidation to acetic acid on VO_x/TiO_2 [7,8]. Reportedly to [9,10], water affects the structure of VO_x species supported on TiO_2 (and other oxides), changing the ratio between polymeric and monomeric species, domain size and coordination environment of vanadium. It is commonly accepted that the promoting effect of water in selective oxidation of functional hydrocarbons on vanadia catalysts is related with two factors: the formation of *V–OH* hydroxyl groups and generation of mobile protons.

The isotopic methods proved to be the most appropriate for elucidating the role of *V–OH* in the mechanism of partial oxidation of hydrocarbons [11,12]. In particular, the isotopic transient study of butene oxidation to acetic acid showed that ^{18}O from $H_2{}^{18}O$ was more readily incorporated into acetic acid than ^{18}O from $^{18}O_2$ [12]. However, the lack of data on the rate of isotope exchange between water and the catalyst oxygen gave no ground for reliable conclusions on the mechanism of these reactions. Taking into account the importance of such studies for a wide range of reactions proceeding on vanadia catalysts, the kinetics of oxygen exchange in the system $H_2O + O_2 + VO_x$ is of special interest.

Our work presents a study of the ^{18}O exchange between H_2O, O_2 and V_2O_5/TiO_2, which was performed under the conditions close to those of selective oxidation of hydrocarbons. The rates of oxygen exchange on two types of the catalyst active sites, *VO* and *VOH*, and the rates of *VO* to *VOH* reversible transformation have been determined.

2. Experimental

2.1. Catalyst

A vanadia–titania oxide catalyst with composition $20\%V_2O_5/80\%TiO_2$ was prepared by impregnation of TiO_2 with a vanadyl oxalate solution. TiO_2 (anatase) with specific surface area of 350 m^2/g was used for the catalyst preparation. The sample was dried in air at 110 °C for 24 h and calcined in an air flow (50 ml/min) at 400 °C for 4 h. The obtained sample was washed with a 10% solution of nitric acid to remove the individual V_2O_5 phase. The sample was calcined once more at 400 °C for 4 h. After washing, the sample contained 7 wt% of vanadium as a monolayer coverage with VO_x particles. Surface area of the sample was 115 m^2/g [13].

2.2. Isotopic experiments

The oxygen isotope exchange experiments were carried out in both the temperature-programmed (TPIE) and isothermal (IIE) modes in a plug-flow reactor (d = 3 mm). The reactor temperature was controlled using a Miniterm-300 heat controller. In all the experiments, 0.2 g catalyst sample was used. The flow rate was 2 ml/s. The chemical and isotopic composition of the gas mixture at the reactor outlet was continuously monitored by a quadrupole mass spectrometer VG SEBSORLAB 200D. Coefficients of relative sensitivity to different components were determined with the appropriate mixtures prepared with helium as a diluent gas.

Prior to each experiment, the catalyst was heated in $1\%O_2 + He$ flow at 300 °C for one hour. Then the catalyst was cooled to 50 °C (TPIE) or 200 °C (IIE) in the same mixture.

Following types of isotopic experiments were performed:

(1) $^{18}O_2/^{16}O_2$ *TPIE in a dry flow*. After the pretreatment, the $1\%O_2$ + He flow was replaced stepwise by the same one containing $^{18}O_2$ ($0.45\%{}^{18}O_2$, $0.55\%{}^{16}O_2$), and the temperature of the sample was raised at a constant rate of 10 K/min up to 500 °C (Fig. 1a).
(2) $^{18}O_2/^{16}O_2$ *TPIE in the presence of water vapor* ($H_2{}^{16}O$). After the pretreatment, the catalyst was kept in $1\%O_2 + 0.6\%H_2O$ + He flow for 20 min. Then this flow was replaced by the same one containing $^{18}O_2$ ($0.45\%{}^{18}O_2$, $0.55\%{}^{16}O_2$), and the temperature of the sample was raised at the rate of 10 K/min up to 500 °C (Fig. 2a).
(3) $H_2{}^{18}O/H_2{}^{16}O$ *TPIE in the presence of dioxygen* ($^{16}O_2$). After the pretreatment, the catalyst was kept in $1\%O_2 + 0.6\%H_2O + He$ flow for 20 min. Then this flow was replaced by the same one containing $H_2{}^{18}O$ (^{18}O enrichment in the water was 75%) and the temperature of the sample was raised at the rate of 10 K/min up to 500 °C (Fig. 3a).
(4) $H_2{}^{18}O/H_2{}^{16}O$ *IIE at* 200 °C *in the presence of dioxygen* ($^{16}O_2$). In contrast to previous case, immediately after the pretreatment $1\%O_2 + He$ flow was replaced by $1\%O_2 + 0.6\%H_2{}^{18}O + He$ one (^{18}O enrichment in the water was 75%).

3. Results and discussion

3.1. Temperature-programmed isotope exchange (TPIE)

3.1.1. TPIE in $^{18}O_2 + {}^{16}O_2$ ($+H_2{}^{16}O$) + He

Figs. 1 and 2 show the experimental profiles and concentrations of oxygen isotope molecules observed at the reactor outlet in a dry flow and in the presence of water vapor, respectively. As seen from the Figures, in both cases, up to the temperature of ca. 400 °C the isotopic distribution of oxygen molecules at the reactor outlet is similar to the isotopic composition of the initial mixture. The concentration of labeled oxygen atoms in water is close to zero (Fig. 2b).

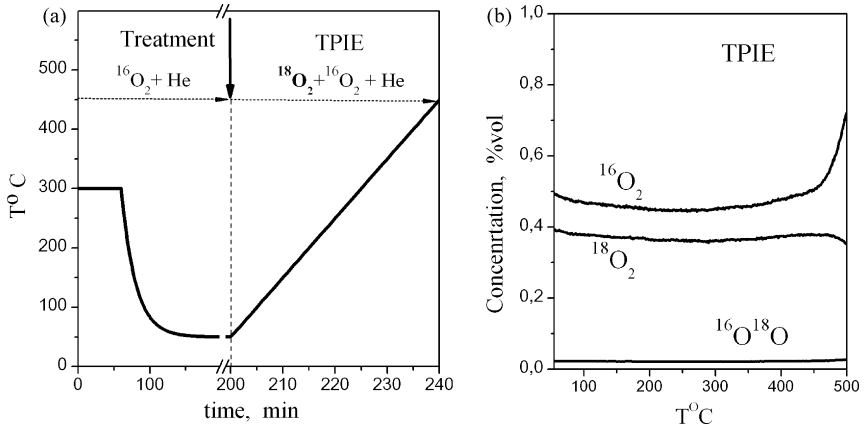

Fig. 1. TPIE in the $0.45\%{}^{18}O_2 + 0.55\%{}^{16}O_2 + He$ flow: (a) experimental profile, (b) concentrations of oxygen isotope molecules at the reactor outlet versus temperature.

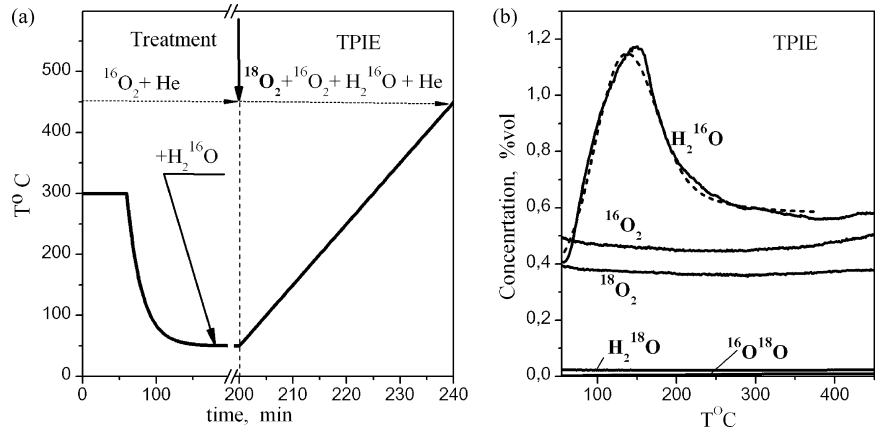

Fig. 2. TPIE in the 0.45%$^{18}O_2$ + 0.55%$^{16}O_2$ + 0.6%$H_2{}^{16}O$ + *He* flow: (a) experimental profile, (b) concentrations of isotope molecules at the reactor outlet (solid lines – experiment, dashed line – calculation).

Thus, at $T < 400\,^{\circ}$C the rate of dioxygen isotope exchange both with the oxide oxygen and with water as well as the rate of dioxygen homoexchange are negligible in comparison with the flow rate. Significant rates of isotope exchange were observed only at $T > 450\,^{\circ}$C, but this led to catalyst reduction, with oxygen released to the gas phase.

Upon catalyst heating in the $O_2 + H_2{}^{16}O$ + He flow (Fig. 2b), a burst of $H_2{}^{16}O$ concentration occurred due to release of water adsorbed during pretreatment at 50 °C. The obtained temperature dependence of the $H_2{}^{16}O$ concentration is described quite well (Fig. 2b, dashed line) by the approximate model of TPR assuming a homogeneous surface:

$$\frac{1}{\beta}\frac{dC_{H_2O}}{dT} = \frac{1}{\tau}(C_{H_2O}^{input} - C_{H_2O}) - b(W_{ADS} - W_{DES}) \quad (1)$$

$$\frac{1}{\beta}\frac{d\theta_{[H_2O]}}{dT} = (W_{ADS} - W_{DES}) \quad (2)$$

$$W_{ADS} = k_{ADS}C_{H_2O}(1 - \theta_{[H_2O]}),\ W_{DES} = \frac{k_{ADS}}{K_R}\theta_{[H_2O]},$$

Here, C_{H_2O} and $\theta_{[H_2O]}$ are the concentrations of water in the gas phase and on the surface, respectively; β is the heating rate; T is the reactor temperature; τ is the contact time; b is the total number of surface sites (mole) per mole of gas molecules present in the catalyst section; k_{ADS} is the rate constant of water adsorption; and $K_R = k_{ADS}/k_{DES}$ is the equilibrium constant.

The temperature dependences of the constants were expressed as follows:

$$k_{ADS} = k_{ADS}^{ref}\, e^{-E_{ADS}/RT'}, \qquad K_R = K_R^{ref}\, e^{Q/RT'}, \qquad T' = \frac{TT^{ref}}{T^{ref} - T},$$

where k_{ADS}^{ref} and K_R^{ref} are values of the constants at a reference temperature T^{ref} taken equal to 200 °C (473 K), E_{ADS} is the activation energy of adsorption, and $Q = (E_{DES} - E_{ADS})$ is the adsorption heat ($Q = -\Delta H$, where ΔH is the adsorption enthalpy).

When solving the inverse problem (1–2), a correlation between k_{ADS}^{ref} and E_{ADS} was found; so the values of these parameters were determined within a rather wide range: $k_{ADS}^{ref} = (1–10)\,s^{-1}$, $E_{ADS} = (5–15)$ kJ/mol. The equilibrium constant was determined more reliably, its value at 200 °C (K_R^{ref}) being 10 (±2), and $Q = 45$ kJ/mol corresponds to that of non-dissociative water adsorption [14]).

3.1.2. TPIE in $H_2{}^{18}O + {}^{16}O_2 + He$

The experimental profiles and results of the experiment are shown in Fig. 3. Similar to the previous case (in the $^{18}O_2 + {}^{16}O_2 + H_2{}^{16}O$ + He flow), first a thermodesorption peak of $H_2{}^{16}O$ was observed. Then the concentration of $H_2{}^{16}O$ decreased, not attaining its level in the initial mixture, and started to increase again. This repeated increase in the $H_2{}^{16}O$ concentration accompanied by a symmetric decrease in the concentration of $H_2{}^{18}O$ can be related to isotope exchange of $H_2{}^{18}O$ with the catalyst oxygen. Note that during this exchange a substitution of the oxide oxygen

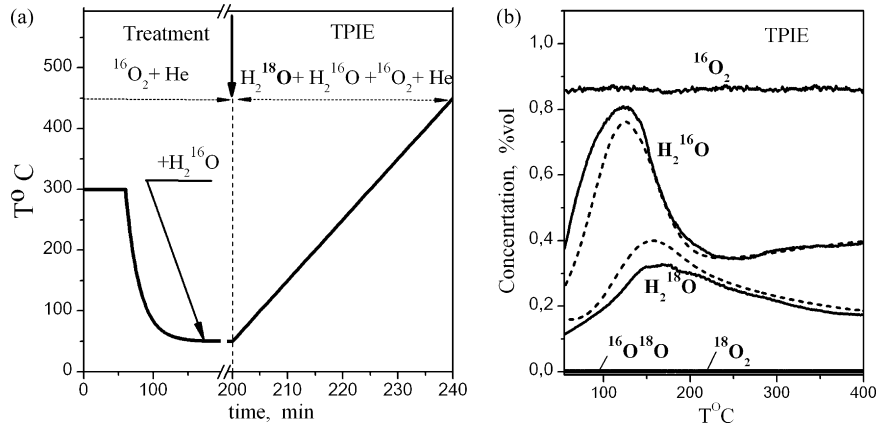

Fig. 3. TPIE in the 0.45%$H_2{}^{18}O$ + 0.15%$H_2{}^{16}O$ + 0.9%$^{16}O_2$ + *He* flow: (a) experimental profile, (b) concentrations of isotope molecules at the reactor outlet (solid lines – experiment, dashed line – calculation).

occurs, but the label does not pass to the gas phase oxygen. Thus, similar to the previous case, the rate of dioxygen exchange with catalyst is negligible.

The oxygen exchange of vanadium oxides with water is known to proceed much more readily than that with dioxygen; this is attributed to a relatively fast reversible adsorption/desorption of water from the surface, whereas the oxygen adsorption is practically irreversible [15,16].

Supplementing the model ((1)–(2)) with equations of isotope exchange (the isotope equations ((3)–(5)) are derived in Appendix A) that describe changes in the fraction of labeled oxygen atoms in water vapor ($\alpha_{H_2O} = H_2^{18}O/(H_2^{16}O + H_2^{18}O)$), adsorbed water ($\alpha_{[H_2O]}$) and catalyst ($\alpha_{Ocat}$):

$$\frac{1}{\beta} C_{H_2O} \frac{\partial \alpha_{H_2O}}{\partial T} = \frac{1}{\tau} C_{H_2O}^{input} (\alpha_{H_2O}^{input} - \alpha_{H_2O}) - bW_{DES}(\alpha_{H_2O} - \alpha_{[H_2O]}) \quad (3)$$

$$\frac{1}{\beta} \theta_{[H_2O]} \frac{\partial \alpha_{[H_2O]}}{\partial T} = W_{ADS}(\alpha_{[H_2O]} - \alpha_{[H_2O]}) - R_{EXCH}(\alpha_{[H_2O]} - \alpha_{Ocat}) \quad (4)$$

$$\frac{1}{\beta} \theta_{Ocat} \frac{\partial \alpha_{Ocat}}{\partial T} = R_{EXCH}(\alpha_{[H_2O]} - \alpha_{Ocat}) \quad (5)$$

where: $R_{EXCH} = k_{EXCH}^{rep}\, e^{-E_{EXCH}/RT'} \theta_{[H_2O]}$, we obtained quite a satisfactory description of the experimental results (Fig. 3, dashed lines) and estimated:

- the amount of exchangeable oxygen in the catalyst: $\theta_{Ocat} \approx 2$ monolayers,
- the rate constant of oxygen exchange between adsorbed water and catalyst at 200 °C: $k_{EXCH}^{rep} = 3(\pm 1) \times 10^{-3}\ s^{-1}$, and
- the activation energy of this exchange: $E_{EXCH} = 68(\pm 3)$ kJ/mol.

Note that E_{EXCH} characterizes the oxygen exchange between adsorbed water and catalyst. However, in the experiment we observe the brutto reaction comprising two steps: the reversible adsorption of water and the proper isotope exchange between adsorbed water and catalyst. It can be shown (see Appendix B) that under the conditions of adsorption/desorption equilibrium at low concentrations of adsorbed water (in this experiment such conditions are implemented at $T > 230$ °C), activation energies of the proper isotope exchange, E_{EXCH}, and brutto reaction, E_{EXCH}^{BRUTTO}, are interrelated by the following equation:

$$E_{EXCH}^{BRUTTO} = E_{EXCH} - Q$$

Substituting the obtained estimates of E_{EXCH} and Q gives $E_{EXCH}^{BRUTTO} = 68 - 45 = 23(\pm 3)$ kJ/mol. Activation energy of the brutto reaction is much lower than the activation energy of proper isotope exchange E_{EXCH}, which explains a relatively weak temperature dependence of the rate of water vapor exchange with the catalyst.

3.2. Isothermal isotope exchange (IIE)

Fig. 4a shows results of the experiment with addition of $H_2{}^{18}O$ in the $^{16}O_2 + He$ mixture passing through the catalyst bed at 200 °C. At zero time (after switching the flows), the outlet concentration of $H_2{}^{16}O$ increases faster than that of $H_2{}^{18}O$. Then, going through a maximum, the concentration of $H_2{}^{16}O$ decreases, while the concentration of $H_2{}^{18}O$ increases over the entire experiment. Since in this case the catalyst was pretreated in a dry flow, the initial concentration of water on the catalyst surface is negligible. Hence, all changes in the isotopic distribution of water molecules are caused by the processes of isotope exchange between water and catalyst oxygen. The dynamic features of this exchange manifest themselves

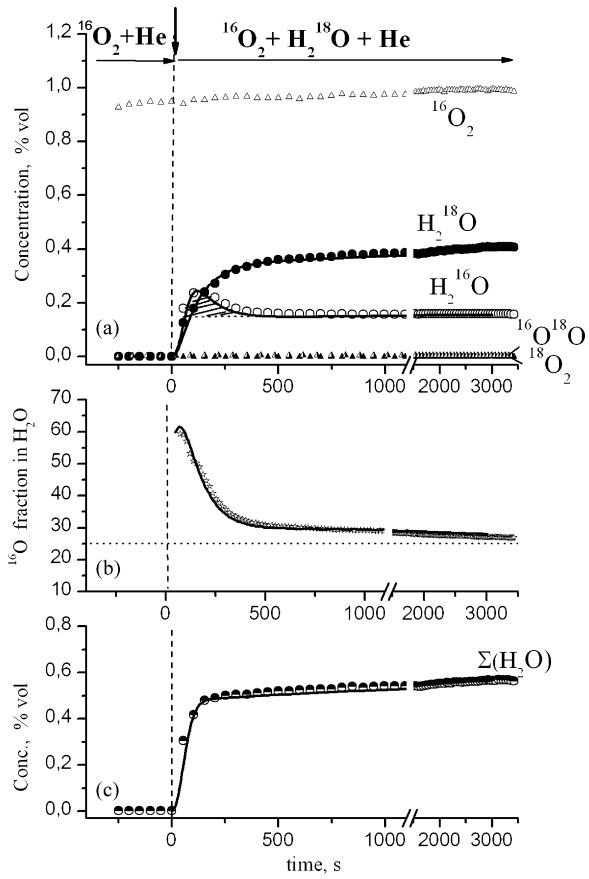

Fig. 4. Time dependences of the concentrations of H_2O and O_2 isotope molecules (a), $H_2{}^{16}O$ fraction (b) and total concentration $\sum H_2O$ (c) after the switch $^{16}O_2 + He \downarrow H_2{}^{18}O + {}^{16}O_2 + He$ (dots – experiment, lines – calculation).

most clearly in the time dependence of ^{16}O isotope fraction in H_2O ($1 - \alpha_{H_2O}$) (Fig. 4b).

At zero time, the rate of isotope exchange between H_2O and catalyst has a maximum value, with the $H_2{}^{16}O$ fraction in water vapor attaining 60% (Fig. 4b). As the catalyst oxygen is substituted by ^{18}O for ^{16}O, the exchange rate decreases and the $H_2{}^{16}O$ fraction approaches its value in the initial mixture (ca. 25%). It is known that isotope exchange on a homogeneous surface is characterized by the exponential dependence of isotope fraction on time. In this case, such dependence resolves into two exponents. Thus, the exchange involves two species of catalyst oxygen differing in the substitution rate. To a first approximation, the amount of rapidly substituted catalyst oxygen can be estimated from the peak area in the $H_2{}^{16}O$ response curve (shaded region):

$$\theta_{[O]fast} = \frac{U}{gS} \int_0^{t_1} (C_{H_2{}^{16}O} - C_{H_2{}^{16}O}^{inlet}) \frac{1}{100} dt \cong 0.04 \times 10^{19}\ [\text{mole/m}^2].$$

Here, U is the flow rate [mole/s], g is the sample weight [g], and S is the specific surface area [m^2/g]).

This value constitutes only a few percent of the monolayer coverage. It is assigned to *V–OH* species, some amount of which may remain on the surface even after a long-term heating of the catalyst. According to the Raman spectroscopy data [15], at temperatures below 230 °C, the hydrogen-bonded surface VO_x species are extensively solvated by water molecules and form a hydrated surface vanadate structure (e.g., decavanadate). We believe that the formation and decomposition of such structures are accompanied by fast isotope exchange between water and *V–OH* species.

As for the slowly substituted catalyst oxygen, its amount exceeds the monolayer coverage. It means that isotope exchange involves both the terminal and bridge oxygen of vanadia. This agrees with the data of [15], indicating that both the *V=O* and bridging *V–O–V* bonds readily undergo oxygen exchange with water vapor. However, the same study [15] reveals that the Raman band of the terminal *V=O* bond of the surface vanadia species on these oxide supports shifts to lower wavenumbers by 5–30 cm^{-1} and becomes broad upon exposure to moisture. Whereas the broad Raman band at ca. 900 cm^{-1}, which is characteristic of the polymeric *V–O–V* functionality, appears to be minimally influenced by the presence of water vapor and is a consequence of the broadness of this band. On this basis we suppose that water interacts directly with *V=O*; thereby, adjacent bridge oxygen is also involved in the isotope exchange. Then, denoting oxygen species, terminal and bridge, by [*VO*], the scheme of oxygen exchange in the system $H_2O + O_2$ + catalyst can be presented as follows:

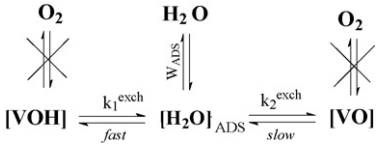

This scheme was used for numerical modeling of experimental response curves. The process model includes nonstationary kinetic equations ((6) and (7)) taking into account changes of water concentration in the gas phase and on the catalyst surface (both with time and along the catalyst bed),

$$\frac{\partial C_{H_2O}}{\partial t} + \frac{1}{\tau}\frac{\partial C_{H_2O}}{\partial \xi} = -b(W_{ADC} - W_{DES}) \quad (6)$$

$$\frac{\partial \theta_{[H_2O]}}{\partial t} = (W_{ADC} - W_{DES}) \quad (7)$$

$$W_{ADC} = k_{ADS} C_{H_2O}(1 - \theta_{[H_2O]})$$
$$W_{DES} = k_{DES}\theta_{[H_2O]}$$

and isotope kinetic equations ((8)–(11)) describing changes of the isotope fraction in water vapor, adsorbed water, [*VOH*] and [*VO*] complexes:

$$C_{H_2O}\left(\frac{\partial \alpha_{H_2O}}{\partial t} + \frac{1}{\tau}\frac{\partial \alpha_{H_2O}}{\partial \xi}\right) = -\beta W_{DES}(\alpha_{H_2O} - \alpha_{[H_2O]}) \quad (8)$$

$$\theta_{[H_2O]}\frac{\partial \alpha_{[H_2O]}}{\partial t} = W_{ADC}(\alpha_{H_2O} - \alpha_{[H_2O]}) - R_1^{exch}(\alpha_{[H_2O]} - \alpha_{[VOH]}) - R_2^{exch}(\alpha_{[H_2O]} - \alpha_{[VO]}) \quad (9)$$

$$\theta_{[VOH]}\frac{\partial \alpha_{[VOH]}}{\partial t} = R_1^{exch}(\alpha_{[H_2O]} - \alpha_{[VOH]}) \quad (10)$$

$$\theta_{[VO]}\frac{\partial \alpha_{[VO]}}{\partial t} = R_2^{exch}(\alpha_{H_2O} - \alpha_{[VO]}) \quad (11)$$

$$R_1 = k_1^{exch}\theta_{[H_2O]}\theta_{[VOH]}$$
$$R_2 = k_2^{exch}\theta_{[H_2O]}\theta_{[VO]}$$

Initial and boundary conditions:

$$t = 0: \quad C_{H_2O} = 0, \quad \theta_{[H_2O]} = 0, \quad \alpha_i = 0,$$
$$\xi = 0: \quad C_{H_2O} = 0.06, \quad \alpha_{[H_2O]} = 0.75$$

The calculated values of rate constants for the oxygen exchange steps, k_1^{exch} and k_2^{exch}, and concentrations of different oxygen species are presented in Table 1, with the corresponding calculated time dependences of ^{16}O fraction in water vapor shown in Fig. 4b.

The value of k_2^{exch} coincides (within the estimation accuracy) with the rate constant for the exchange between adsorbed water and catalyst, k_{EXCH}, which was determined from the TPIE data. This allows assigning the activation energy E_{EXCH} exactly to the exchange with [*VO*] sites (*V=O* and *V–O–V*). As for the [*VOH*] sites, most likely they are substituted at lower temperatures and dynamics of this process is overridden by thermodesorption of water. It means that the activation energy of isotope exchange with [*VOH*] is very low (much lower than E_{EXCH}).

The calculation allowed us to make the following conclusion: to provide the rate of isotope exchange between H_2O and catalyst corresponding to the rate observed in the initial period of time in experiment, rate constants of water adsorption and desorption should be equal to $k_{ADS} \geq 1$ and $k_{DES} \geq 0.1\ s^{-1}$. At such values of rate constants, the time of establishing the adsorption–desorption equilibrium does not exceed 100 s. By this time, the calculated concentration of water in the gas phase ($\sum H_2O$) becomes constant and equal to its concentration in the initial mixture, whereas in the experiment it is somewhat (by ca. 5–10%) lower than the initial value and later increases very slowly (Fig. 4c). Thus, along with fast reversible non-dissociative adsorption of water, there is a slow process, which seems to relate with the formation of additional amount of *VOH* species.

According to [17], surface V^{5+} coordinates the *OH* group as complexes

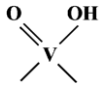

which can be dehydrated at high temperatures. The formation mechanism for these complexes can be presented as

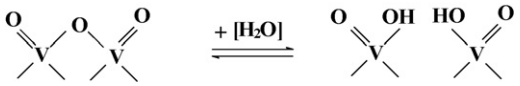

Supplementing the model ((6)–(11)) with an equation that takes into account changes in the concentration of [*VOH*]:

$$\frac{\partial \theta_{[VOH]}}{\partial t} = 2W_{[VOH]},$$

where $W_{[VOH]} = k^{+}_{VOH}\theta_{[H_2O]}(1 - \theta_{[VOH]}) - k^{-}_{VOH}\theta_{[VOH]}$, and introducing the expression for W_{VOH} into Eq. (7), we obtained a complete description of changes in both the total concentration of water vapor with time (Fig. 4a) and the concentration of isotope molecules $H_2{}^{16}O$ and $H_2{}^{18}O$ (Fig. 4a). The corresponding values of rate constants for the steps of water interaction with catalyst are listed in Table 2.

According to the model calculations, the concentration of [*VOH*] sites increased from 4% to 15(±5)% for the time corresponding to duration of the experiment (3000 s). However, it did not attain the equilibrium concentration, which is equal to ca. 20%. By our estimates, the representative time of transition to a new equilibrium state is ca. 10^4 s.

As seen from Tables 1 and 2, rate constant of the isotope exchange between [H_2O] and [*VO*] (k_{2eff}^{exch}) coincides by the order of magnitude with the rate constant of the [*VOH*] sites formation (k^{+}_{VOH}). It is reasonable to assume that these processes are interrelated; thus, the isotope exchange of water with terminal and bridge oxygen occurs during formation and decomposition of the [*VOH*] sites. A possible variant of the mechanism of such exchange is shown below:

Table 1
Kinetic parameters of the oxygen exchange between adsorbed water and the catalyst oxygen.

$[H_2O] \leftrightarrow [VOH]$			$[H_2O] \leftrightarrow [VO]$		
k_1^{exch} [s^{-1}]	E_1^{exch} [kJ/mol]	θ_{VOH} [% of monolayer]	k_2^{exch} [s^{-1}]	E_2^{exch} [kJ/mol]	$\theta_{[VO]}$ [% of monolayer]
0.5	Very low	4(±0.5)	$2(\pm0.5)\times10^{-3}$	70	ca. 200

Table 2
Rate constants for the steps of water–catalyst interaction.

$H_2O \leftrightarrow [H_2O]$		$[H_2O]+[VO(V)] \leftrightarrow 2[VOH]$	
k_{ADS} [s^{-1}]	k_{DES} [s^{-1}]	k^{+}_{VOH} [s^{-1}]	k^{-}_{VOH} [s^{-1}]
2(±0.5)	$2(\pm0.5)\times10^{-1}$	$4(\pm1)\times10^{-3}$	$1(\pm0.5)\times10^{-3}$

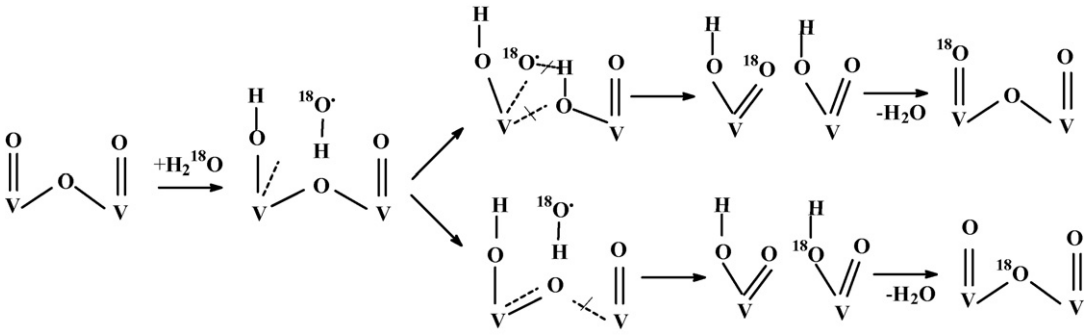

Unlike the exchange between $[H_2O]$ and $[VOH]$, the mechanism of this exchange implies cleavage and formation of new chemical bonds. This explains a comparatively high activation energy of such exchange.

Results obtained in our study allow us to explain some effects of water vapor on the kinetics of hydrocarbon oxidations. In particular, when 1-butene is oxidized at 160–200 °C, the introduction of water vapor into reaction mixture led first to a sharp spike of the concentration of partial oxidation products and then to a slow increase in the concentration of target product, acetic acid [12]. The representative time of transition to a new stationary state was ca. 10^4 s, which coincides with representative time of the sites transformation. On this basis, we conclude that slow relaxations observed in this reaction are related with increasing concentration of *V–OH* sites, while fast relaxations are related with adsorption of water, which displaces the reaction products from the surface. The same concept can explain the effect of water on the oxidation of toluene over vanadium oxide catalysts [5]. After removal of water from the reaction mixture, the rate of toluene oxidation decreased, but not down to the original level before water addition. In line with this assumption, a prolonged effect of water is related most likely with hydrolysis of *V–O–V* bonds by water. We believe that during the oxidation of β-picoline the positive effect of water is caused by increasing the number of Brønsted sites. Our previous experiments revealed two species of adsorbed picoline, hydrogen-bonded and coordinatively bound with the Levis acid sites, on vanadia–titania catalysts [18]. A strong dependence of the rate of β-picoline oxidation on the concentration of water vapor [1] is attributed to an increase in the surface concentration of β-picoline species which are hydrogen-bonded to the *V–OH* sites.

The above examples show that adsorption of water and transformation of the sites may produce the additive effect on the rate of partial oxidation of hydrocarbons.

4. Conclusion

Unlike dioxygen, water can exchange quite readily its oxygen atoms with VO_x supported on TiO_2. Surface sites coordinating the *OH* group show the highest activity in the oxygen exchange with water. The rate constant of oxygen exchange between adsorbed water molecule and *V–OH* is ca. 0.5 s^{-1} at 200 °C, with the activation energy close to zero. The rate of oxygen exchange with dehydrated vanadium complexes *V–O–V* and *V=O* is much lower. The rate constant of this exchange is ca. 10^{-3} s^{-1} at 200 °C, with the activation energy of ca. 70 kJ/mol. The interaction of adsorbed water with VO_x species results in hydrolysis of vanadia sites to form the *V–OH* groups, which recombination underlies the isotope exchange.

Appendix A. A mathematical model of the temperature-programmed isotope exchange under non-equilibrium conditions

In distinction to the known isotope kinetic models based on the conditions of adsorption–desorption equilibrium, in this case it is necessary to take into account changes not only in the isotopic composition, but also in the concentration of substances involved in the isotope exchange.

Let us consider the isotope exchange between water vapor and catalyst as a two-step reaction comprising the steps of adsorption and interaction between adsorbed water and catalyst oxygen accompanied by the exchange of their oxygen atoms. Then, the temperature dependences of labeled water concentrations in the gas phase and on the surface will be described by a set of equations:

$$\frac{1}{\beta}\frac{\partial C_{H_2{}^{18}O}}{\partial T} = \frac{1}{\tau}(C^{input}_{H_2{}^{18}O} - C_{H_2{}^{18}O}) - b(k_{ADS}C_{H_2{}^{18}O}(1-\theta_{[H_2O]}) - k_{DES}\theta_{[H_2{}^{18}O]}) \quad (A.1)$$

$$\frac{1}{\beta}\frac{\partial \theta_{[H_2{}^{18}O]}}{\partial T} = (k_{ADS}C_{[H_2{}^{18}O]}(1-\theta_{H_2O}) - k_{DES}\theta_{[H_2{}^{18}O]}) - k_{EXCH}\theta_{[H_2{}^{18}O]}\theta_{[{}^{16}O_{Cat}]} + k_{EXCH}\theta_{[H_2{}^{16}O]}\theta_{[{}^{18}O_{Cat}]} \quad (A.2)$$

$$\frac{1}{\beta}\frac{\partial \theta_{[{}^{18}O_{Cat}]}}{\partial T} = k_{EXCH}\theta_{[H_2{}^{18}O]}\theta_{[{}^{16}O_{Cat}]} - k_{EXCH}\theta_{[H_2{}^{16}O]}\theta_{[{}^{18}O_{Cat}]} \quad (A.3)$$

Expressing $C_{H_2{}^{18}O}$, $\theta_{[H_2{}^{18}O]}$ and $\theta_{[{}^{18}O_{Cat}]}$ as

$$C_{H_2{}^{18}O} = C_{H_2O}\alpha_{H_2O}$$

$$\theta_{[H_2{}^{18}O]} = \theta_{[H_2O]}\alpha_{[H_2O]}$$

$$\theta_{[{}^{18}O_{Cat}]} = \theta_{[O_{Cat}]}\alpha_{[O_{Cat}]}$$

and substituting these expressions into the set of Eqs. ((A.1)–(A.3)) give:

$$\frac{1}{\beta}\left(C_{H_2O}\frac{\partial\alpha_{H_2O}}{\partial T} + \alpha_{H_2O}\frac{\partial C_{H_2O}}{\partial T}\right) = \frac{1}{\tau}(C_{H_2O}^{input}\alpha_{H_2O}^{input} - C_{H_2{}^{18}O}\alpha_{H_2O}) - b(W_{ADS}\alpha_{[H_2O]} - W_{DES}\alpha_{[H_2O]}) \quad (A.4)$$

$$\frac{1}{\beta}(\theta_{[H_2O]}\frac{\partial\alpha_{[H_2O]}}{\partial T} + \alpha_{[H_2O]}\frac{\partial\theta_{[H_2O]}}{\partial T}) = (W_{ADS}\alpha_{H_2O} - W_{DES}\alpha_{[H_2O]}) - R_{EXCH}(\alpha_{[H_2O]}(1-\alpha_{[O_{Cat}]}) - \alpha_{[O_{Cat}]}(1-\alpha_{[H_2O]})) \quad (A.5)$$

$$\frac{1}{\beta}\theta_{[O_{Cat}]}\frac{\partial\alpha_{[O_{Cat}]}}{\partial T} = R_{EXCH}(\alpha_{[H_2O]}(1-\alpha_{[O_{Cat}]}) - \alpha_{[O_{Cat}]}(1-\alpha_{[H_2O]})) \quad (A.6)$$

Then dC_{H_2O}/dT and $\partial\theta_{[H_2O]}/\partial T$ are expressed from Eqs. (1) and (2) as

$$\frac{dC_{H_2O}}{dT} = \beta\left[\frac{1}{\tau}(C_{H_2O}^{input} - C_{H_2O}) - b(W_{ADS} - W_{DES})\right]$$

$$\frac{d\theta_{[H_2O]}}{dT} = \beta[W_{ADS} - W_{DES}]$$

and substituted in ((A.4.)–(A.5.)):

$$\frac{1}{\beta}C_{H_2O}\frac{\partial\alpha_{H_2O}}{\partial T} + \alpha_{H_2O}\left[\frac{1}{\tau}(C_{H_2O}^{input} - C_{H_2O}) - b(W_{ADS} - W_{DES})\right] = \frac{1}{\tau}(C_{H_2O}^{input}\alpha_{H_2O}^{input} - C_{H_2{}^{18}O}\alpha_{H_2O}) - b(W_{ADS}\alpha_{[H_2O]} - W_{DES}\alpha_{[H_2O]}) \quad (A.7)$$

$$\frac{1}{\beta}\theta_{[H_2O]}\frac{\partial\alpha_{[H_2O]}}{\partial T} + \alpha_{[H_2O]}[W_{ADS} - W_{DES}] = (W_{ADS}\alpha_{H_2O} - W_{DES}\alpha_{[H_2O]}) - R_{EXCH}(\alpha_{[H_2O]}(1-\alpha_{[O_{Cat}]}) - \alpha_{[O_{Cat}]}(1-\alpha_{[H_2O]}) \quad (A.8)$$

And finally, a little identical transformation brings Eqs. ((A.7)–(A.8)) and Eq. (A.6) to the form:

$$\frac{1}{\beta}C_{H_2O}\frac{\partial\alpha_{H_2O}}{\partial T} = \frac{1}{\tau}C_{H_2O}^{input}(\alpha_{H_2O}^{input} - \alpha_{H_2O}) - bW_{DES}(\alpha_{H_2O} - \alpha_{[H_2O]})$$

$$\frac{1}{\beta}\theta_{[H_2O]}\frac{\partial\alpha_{[H_2O]}}{\partial T} = W_{ADS}(\alpha_{H_2O} - \alpha_{[H_2O]}) - R_{EXCH}(\alpha_{[H_2O]} - \alpha_{Ocat})$$

$$\frac{1}{\beta}\theta_{Ocat}\frac{\partial\alpha_{Ocat}}{\partial T} = R_{EXCH}(\alpha_{[H_2O]} - \alpha_{Ocat})$$

Appendix B. A ratio between activation energies of the brutto reaction (adsorption + isotope exchange) and the proper isotope exchange on the catalyst surface

Let us consider a set of Eqs. (3)–(5), which was used for TPIE modeling.

$$\frac{1}{\beta}C_{H_2O}\frac{\partial\alpha_{H_2O}}{\partial T} = \frac{1}{\tau}C_{H_2O}^{input}(\alpha_{H_2O}^{input} - \alpha_{H_2O}) - bW_{DES}(\alpha_{H_2O} - \alpha_{[H_2O]}) \quad (B.1)$$

$$\frac{1}{\beta}\theta_{[H_2O]}\frac{\partial\alpha_{[H_2O]}}{\partial T} = W_{ADS}(\alpha_{H_2O} - \alpha_{[H_2O]}) - R_{EXCH}(\alpha_{[H_2O]} - \alpha_{Ocat}) \quad (B.2)$$

$$\frac{1}{\beta}\theta_{Ocat}\frac{\partial\alpha_{Ocat}}{\partial T} = R_{EXCH}(\alpha_{[H_2O]} - \alpha_{Ocat}) \quad (B.3)$$

Let us assume that the exchange proceeds under the conditions close to adsorption–desorption equilibrium ($W_{ADS} = W_{DES}$), and concentration of adsorbed water $\theta_{[H_2O]}$ is negligible in comparison with θ_{Ocat} and C_{H_2O}. Then, using a quasistationary approximation for $\theta_{[H_2O]}$, the system can be transformed into the following form.

$$\frac{1}{\beta}C_{H_2O}\frac{\partial\alpha_{H_2O}}{\partial T} = \frac{1}{\tau}C_{H_2O}^{input}(\alpha_{H_2O}^{input} - \alpha_{H_2O}) - bW_{ADS}(\alpha_{H_2O} - \alpha_{[H_2O]}) \quad (B.4)$$

$$0 = W_{ADS}(\alpha_{H_2O} - \alpha_{[H_2O]}) - R_{EXCH}(\alpha_{[H_2O]} - \alpha_{Ocat}) \quad (B.5)$$

$$\frac{1}{\beta}\theta_{Ocat}\frac{\partial\alpha_{Ocat}}{\partial T} = R_{EXCH}(\alpha_{[H_2O]} - \alpha_{Ocat}) \quad (B.6)$$

Expressing $\alpha_{[H_2O]}$ from (B.5) and substituting into (B.4) and (B.6) give:

$$\frac{1}{\beta}C_{H_2O}\frac{\partial\alpha_{H_2O}}{\partial T} = \frac{1}{\tau}C_{H_2O}^{input}(\alpha_{H_2O}^{input} - \alpha_{H_2O}) - b\frac{R_{EXCH}}{1+R_{EXCH}/W_{ADS}}(\alpha_{H_2O} - \alpha_{[Ocat]}) \quad (B.7)$$

$$\frac{1}{\beta}\theta_{Ocat}\frac{\partial\alpha_{Ocat}}{\partial T} = \frac{R_{EXCH}}{1+R_{EXCH}/W_{ADS}}(\alpha_{[H_2O]} - \alpha_{Ocat}) \quad (B.8)$$

where $R_{EXCH}/(1+R_{EXCH}/W_{ADS})$ is the rate of the brutto reaction, R_{BRUTTO}.

Substituting into R_{BRUTTO} the expressions for step rates R_{EXCH} and W_{ADS} and taking into account that $\theta_{[H_2O]} = K_R C_{H_2O}$, we obtain:

$$R_{BRUTTO} = \frac{k_{EXCH}K_R C_{H_2O}}{1 + k_{EXCH}K_R/k_{ADS}} \approx k_{EXCH}K_R C_{H_2O} \quad (since\, k_{ADS} >> k_{EXCH}K_R),$$

where $k_{EXCH}k_R$ is the effective rate constant of the brutto-reaction, k_{BRUTTO}.

Thus, we obtain: $k_{BRUTTO} \approx k_{EXCH}^{rep}e^{-E_{EXCH}/RT'}K_R^{rep}\,e^{Q/RT'} = k_{EXCH}^{rep}K_R^{rep}e^{-E_{EXCH}-Q/RT'}$, i.e., activation energy of the brutto reaction is equal to $E_{EXCH}^{BRUTTO} \approx E_{EXCH} - Q$.

References

[1] E.V. Ovchinnikova, T.V. Andrushkevich, L.A. Shadrina, React. Kinet. Catal. Lett. 82 (1) (2004) 191–197.
[2] K. Takehira, T. Shishido, Z. Song, T. Matsushita, T. Kawabata, K. Takaki, Catal. Today 91/92 (2004) 7–11.
[3] T. Shishido, Z. Song, T. Matsushita, K. Takaki, K. Takehira, Phys. Chem. Chem. Phys. 5 (2003) 2710–2718.
[4] C.-H. Lin, H. Bai, Appl. Catal. B 42 (2003) 279–287.
[5] J. Zhu, S. Lars, T. Andersson, Appl. Catal. 53 (1989) 251–262.
[6] M. Antol, A. Kaszonyi, M. Hronec, Collect. Czech. Chem. Commun. 61 (1996) 1675–1680.

[7] K. Kaneko, T. Koyama, S. Wada, Bull. Jpn. Petr. Inst. 16 (1974) 17–23.
[8] T. Seiyama, K. Nita, T. Maehara, N. Yamazoe, Y. Takita, J. Catal. 49 (1977) 164–173.
[9] B. Olthof, A. Khodakov, A.T. Bell, E. Iglesia, J. Phys. Chem. B 104 (2000) 1516–1528.
[10] V.A. Ranea, J.L. Vicente, E.E. Mola, P. Arnal, H. Thomas, L. Gambaro, Surf. Sci. 463 (2000) 115–124.
[11] H.W. Zanthoff, M. Sananes-Schultz, S.A. Buchholz, U. Rodemerck, B. Kubias, M. Baerns, Appl. Catal. A: Gen. 172 (1998) 49–58.
[12] W.Y. Suprun, D.P. Sabde, H.-K. Schädlich, B. Kubias, H. Papp, Appl. Catal. A. Gen. 289 (2006) 66–73.
[13] G.Ya. Popova, T.V. Andrushkevich, E.V. Semionova, Yu.A. Chesalov, L.S. Dovlitova, V.A. Rogov, V.N. Parmon, J. Mol. Catal. A: Chem. 283 (2008) 146–152.
[14] T.E. Madey, J.T. Yates Jr., Chem. Phys. Lett. 51 (1977) 77–83.
[15] J.-M. Jehng, G. Deo, B.M. Weckhuysen, I.E. Wachs, J. Mol. Catal. A Chem. 110 (1996) 41–54.
[16] K. Chen, A. Khodakov, J. Yang, A.T. Bell, E. Iglesia, J. Catal. 186 (1999) 325–333.
[17] B.S. Balzhinimaev, L.G. Pinaeva, Kinet. Catal. 36 (1995) 60.
[18] G.Ya. Popova, T.V. Andrushkevich, Y.A. Chesalov, E.V. Ovchinnikova, React. Kinet. Catal. Lett. 87 (2006) 387–394.